Diffuse radiation forcing constraints on gross primary productivity and global terrestrial evapotranspiration – Supporting Information

T. Chakraborty[1,2*], X. Lee[2], and D. M. Lawrence[3]

[1]Pacific Northwest National Laboratory, Richland, WA, USA

[2]Yale School of the Environment, CT, USA

[3]National Center for Atmospheric Research, CO, USA

---

*Corresponding author: T. Chakraborty, Email:tc.chakraborty@pnnl.gov

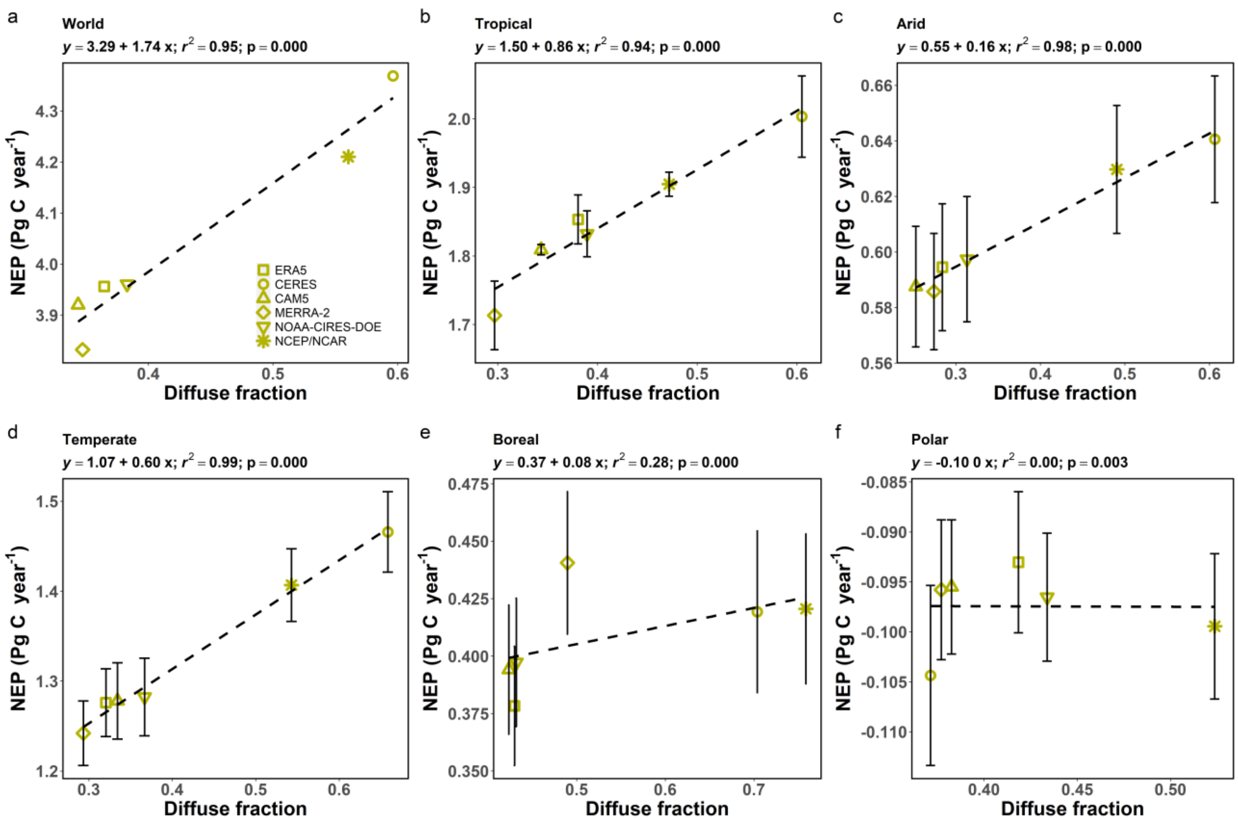

Figure S1 Response of net ecosystem productivity to inter-product diffuse fraction spread. Associations between net ecosystem productivity (NEP) and diffuse fraction (k_d) across different land model simulations forced using k_d from the six products (NCEP/NCAR, NOAA-CIRES-DOE, ERA5, MERRA-2, CERES, and CAM; represented using different symbols) considered here for (a) all terrestrial surfaces, (b) tropical climate, (c) arid climate, (d) temperate climate, (e) boreal climate, and (f) polar climate. The lines of best fit and the linear regression equations, with coefficient of determination r^2 and p-values are noted. The vertical error bars show the inter-annual standard error for the 10-year period.

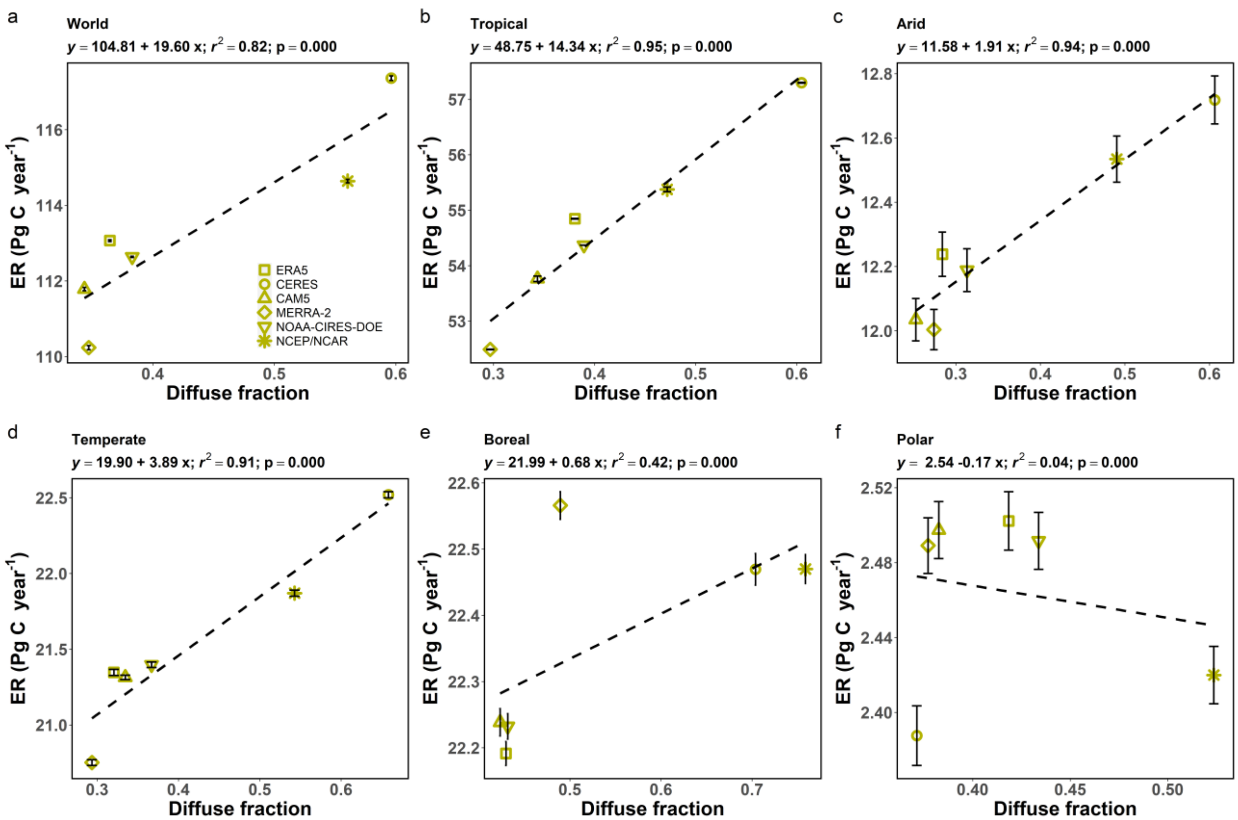

Figure S2 Response of ecosystem respiration to inter-product diffuse fraction spread. Associations between ecosystem respiration (ER) and diffuse fraction (k_d) across different land model simulations forced using k_d from the six products (NCEP/NCAR, NOAA-CIRES-DOE, ERA5, MERRA-2, CERES, and CAM; represented using different symbols) considered here for (a) all terrestrial surfaces, (b) tropical climate, (c) arid climate, (d) temperate climate, (e) boreal climate, and (f) polar climate. The lines of best fit and the linear regression equations, with coefficient of determination r^2 and p-values are noted. The vertical error bars show the inter-annual standard error for the 10-year period.

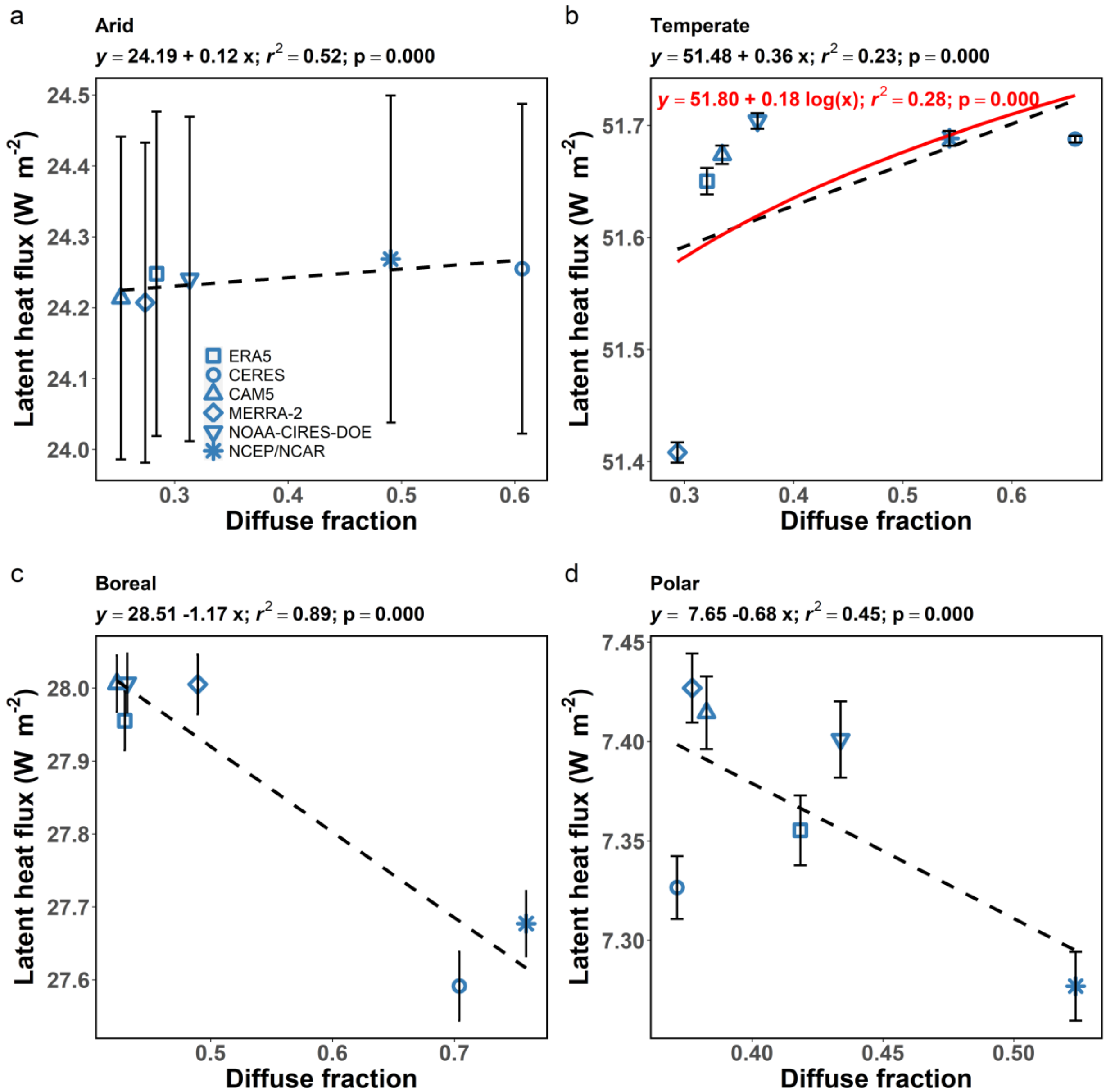

Figure S3 Response of latent heat flux to inter-product diffuse fraction spread. Associations between latent heat flux and diffuse fraction (k_d) across different land model simulations forced using k_d from the six products (NCEP/NCAR, NOAA-CIRES-DOE, ERA5, MERRA-2, CERES, and CAM; represented using different symbols) considered here for (a) arid climate, (b) temperate climate, (c) boreal climate, and (d) polar climate. The lines of best fit and the linear regression equations, with coefficient of determination r^2 and p-values are noted. For temperate climate, (a) logarithmic fit and the associated equation is also noted (in red). The vertical error bars show the inter-annual standard error for the 10-year period.

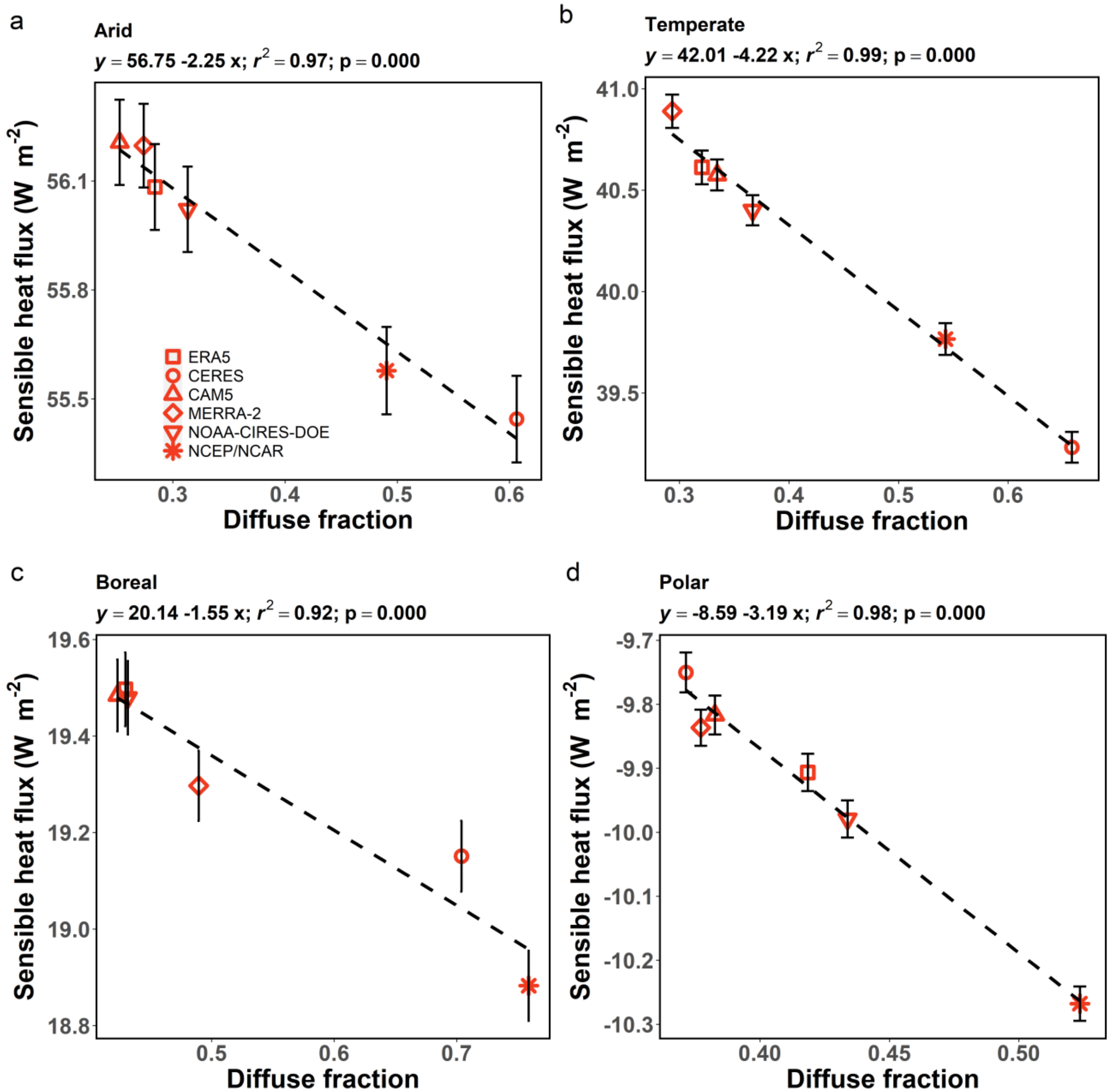

Figure S4 Response of sensible heat flux to inter-product diffuse fraction spread. Associations between sensible heat flux and diffuse fraction (k_d) across different land model simulations forced using k_d from the six products (NCEP/NCAR, NOAA-CIRES-DOE, ERA5, MERRA-2, CERES, and CAM; represented using different symbols) considered here for (a) arid climate, (b) temperate climate, (c) boreal climate, and (d) polar climate. The lines of best fit and the linear regression equations, with coefficient of determination r^2 and p-values are noted. The vertical error bars show the inter-annual standard error for the 10-year period.

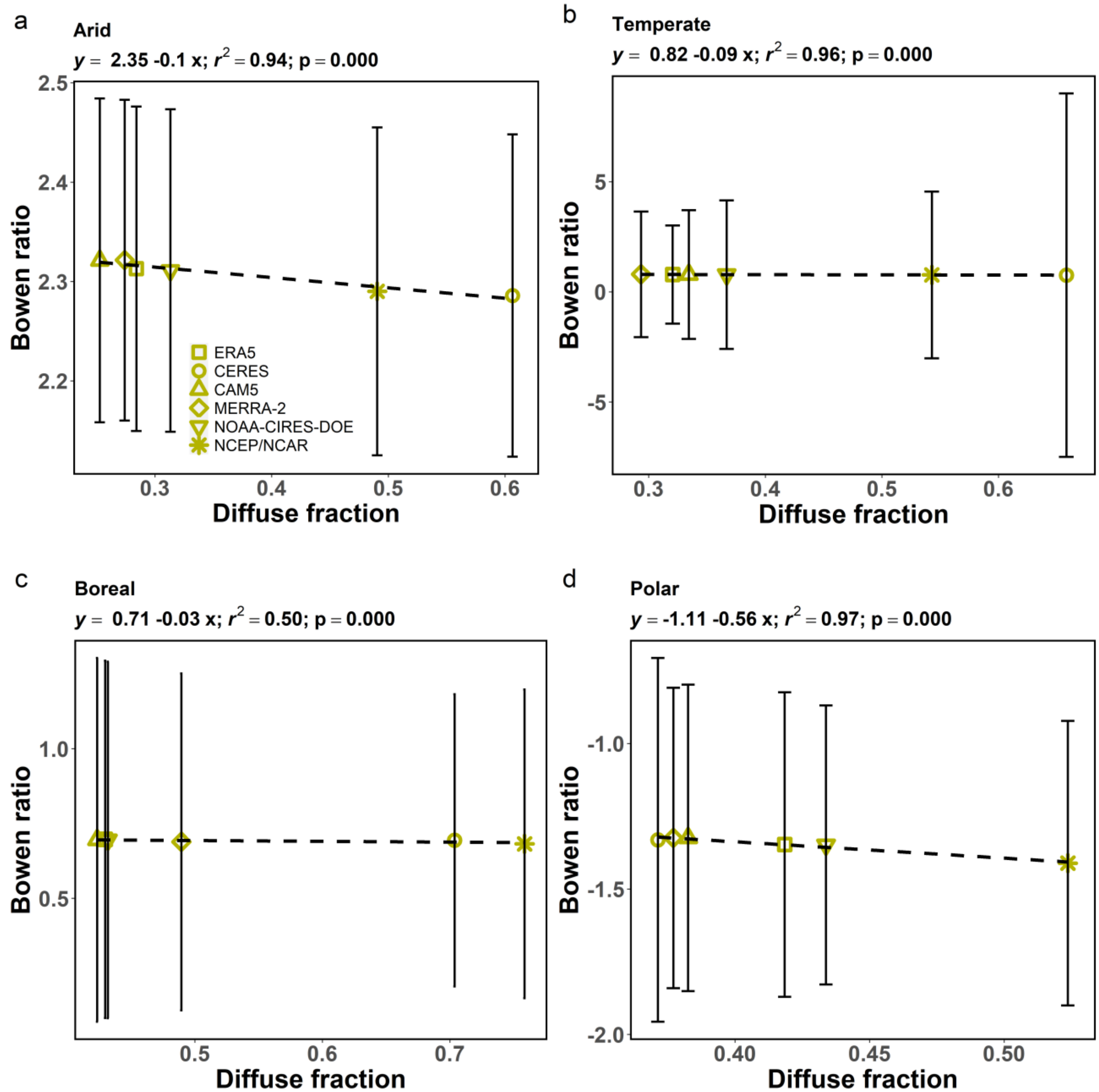

Figure S5 Response of Bowen ratio to inter-product diffuse fraction spread. Associations between Bowen ratio and diffuse fraction (k_d) across different land model simulations forced using k_d from the six products (NCEP/NCAR, NOAA-CIRES-DOE, ERA5, MERRA-2, CERES, and CAM) considered here for (a) arid climate, (b) temperate climate, (c) boreal climate, and (d) polar climate. The lines of best fit and the linear regression equations, with coefficient of determination r^2 and p-values are noted. The vertical error bars show the inter-annual standard error for the 10-year period.

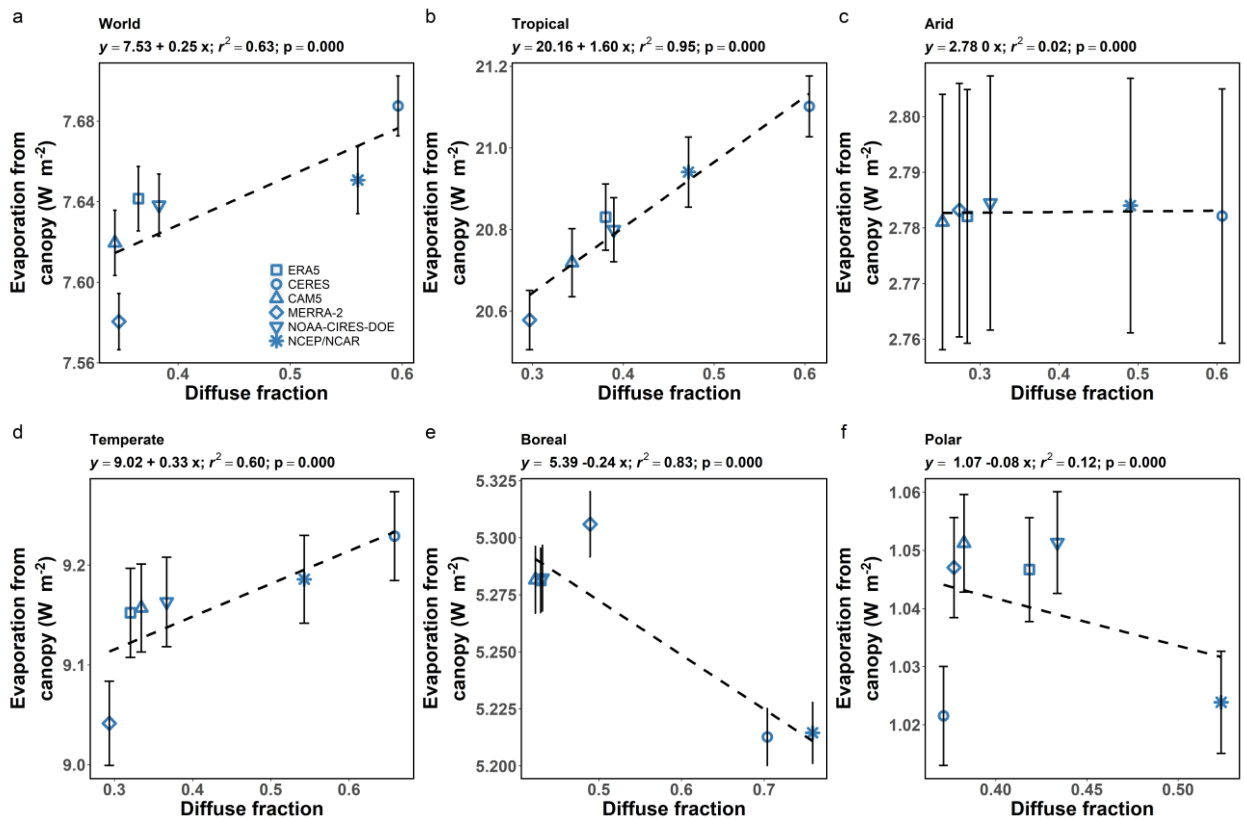

Figure S6 Response of evaporation from canopy to inter-product diffuse fraction spread. Associations between evaporation from canopy and diffuse fraction (k_d) across different land model simulations forced using k_d from the six products (NCEP/NCAR, NOAA-CIRES-DOE, ERA5, MERRA-2, CERES, and CAM; represented using different symbols) considered here for (a) all terrestrial surfaces, (b) tropical climate, (c) arid climate, (d) temperate climate, (e) boreal climate, and (f) polar climate. The lines of best fit and the linear regression equations, with coefficient of determination r^2 and p-values are noted. The vertical error bars show the inter-annual standard error for the 10-year period.

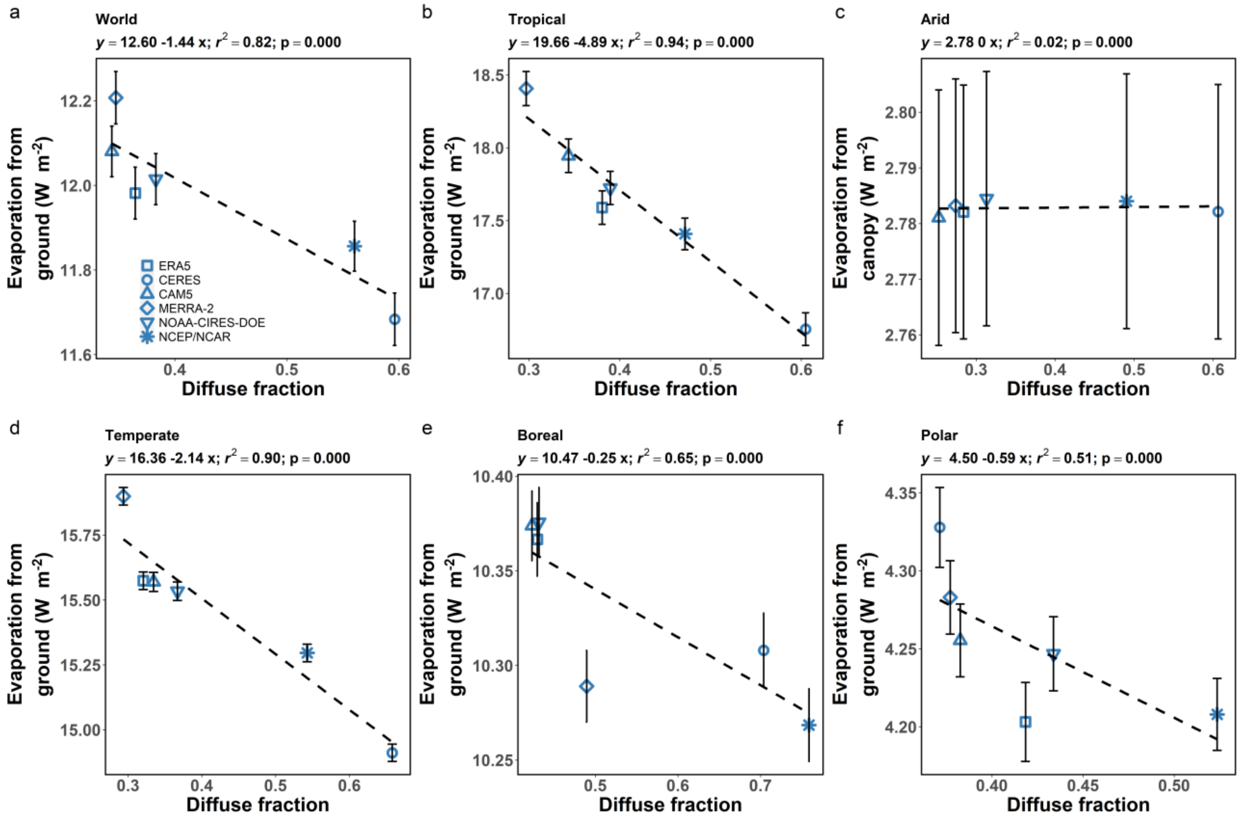

Figure S7 Response of evaporation from ground to inter-product diffuse fraction spread. Associations between evaporation from ground and diffuse fraction (k_d) across different land model simulations forced using k_d from the six products (NCEP/NCAR, NOAA-CIRES-DOE, ERA5, MERRA-2, CERES, and CAM; represented using different symbols) considered here for (a) all terrestrial surfaces, (b) tropical climate, (c) arid climate, (d) temperate climate, (e) boreal climate, and (f) polar climate. The lines of best fit and the linear regression equations, with coefficient of determination r^2 and p-values are noted. The vertical error bars show the inter-annual standard error for the 10-year period.

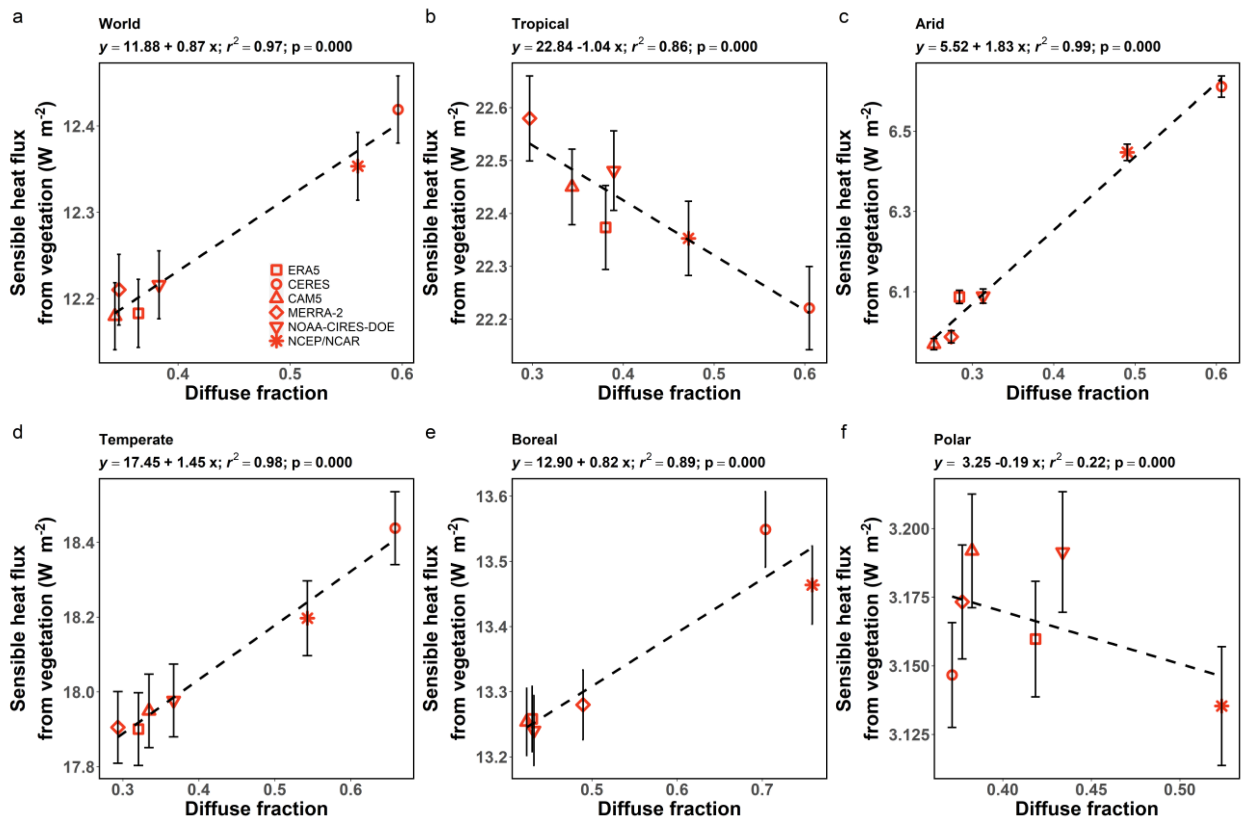

Figure S8 Response of sensible heat flux from vegetation to inter-product diffuse fraction spread. Associations between sensible heat flux from vegetation and diffuse fraction (k_d) across different land model simulations forced using k_d from the six products (NCEP/NCAR, NOAA-CIRES-DOE, ERA5, MERRA-2, CERES, and CAM; represented using different symbols) considered here for (a) all terrestrial surfaces, (b) tropical climate, (c) arid climate, (d) temperate climate, (e) boreal climate, and (f) polar climate. The lines of best fit and the linear regression equations, with coefficient of determination r^2 and p-values are noted. The vertical error bars show the inter-annual standard error for the 10-year period.

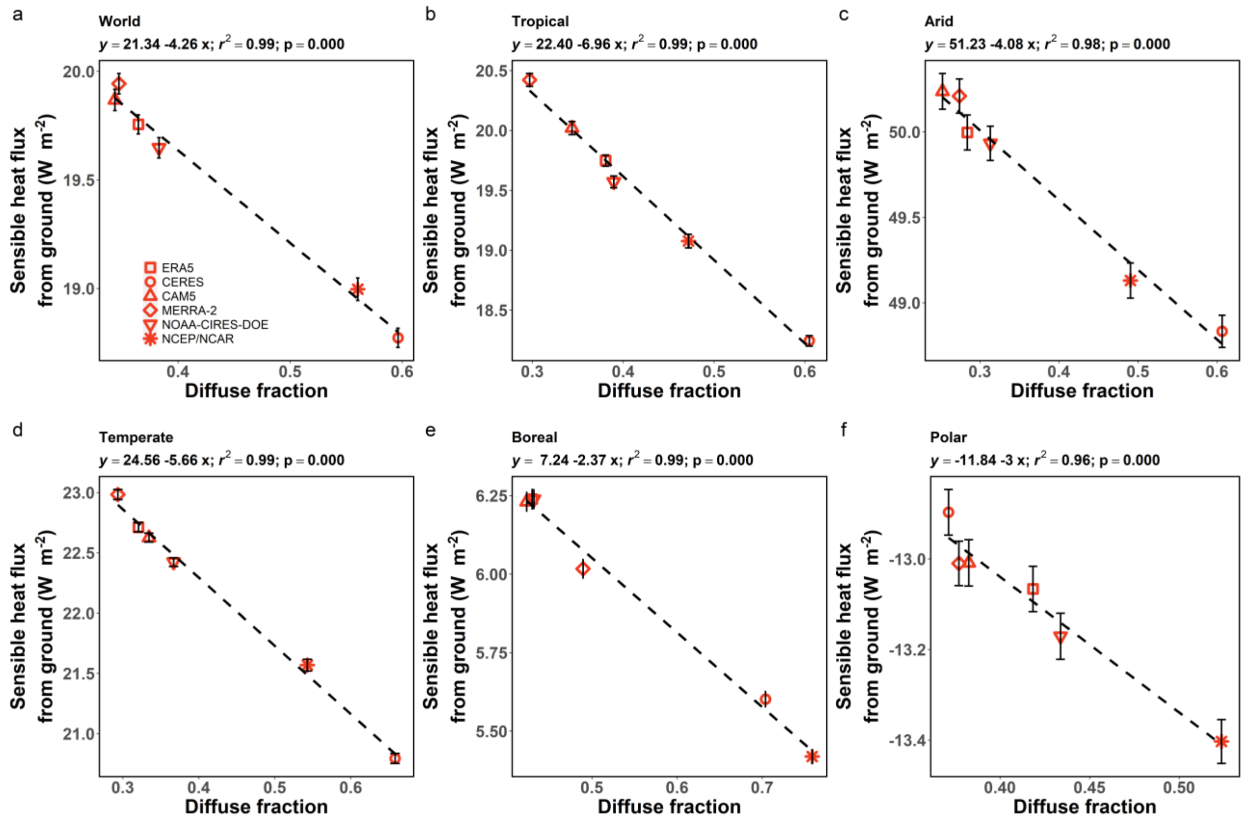

Figure S9 Response of sensible heat flux from ground to inter-product diffuse fraction spread. Associations between sensible heat flux from ground and diffuse fraction (k_d) across different land model simulations forced using k_d from the six products (NCEP/NCAR, NOAA-CIRES-DOE, ERA5, MERRA-2, CERES, and CAM; represented using different symbols) considered here for (a) all terrestrial surfaces, (b) tropical climate, (c) arid climate, (d) temperate climate, (e) boreal climate, and (f) polar climate. The lines of best fit and the linear regression equations, with coefficient of determination r^2 and p-values are noted. The vertical error bars show the inter-annual standard error for the 10-year period.

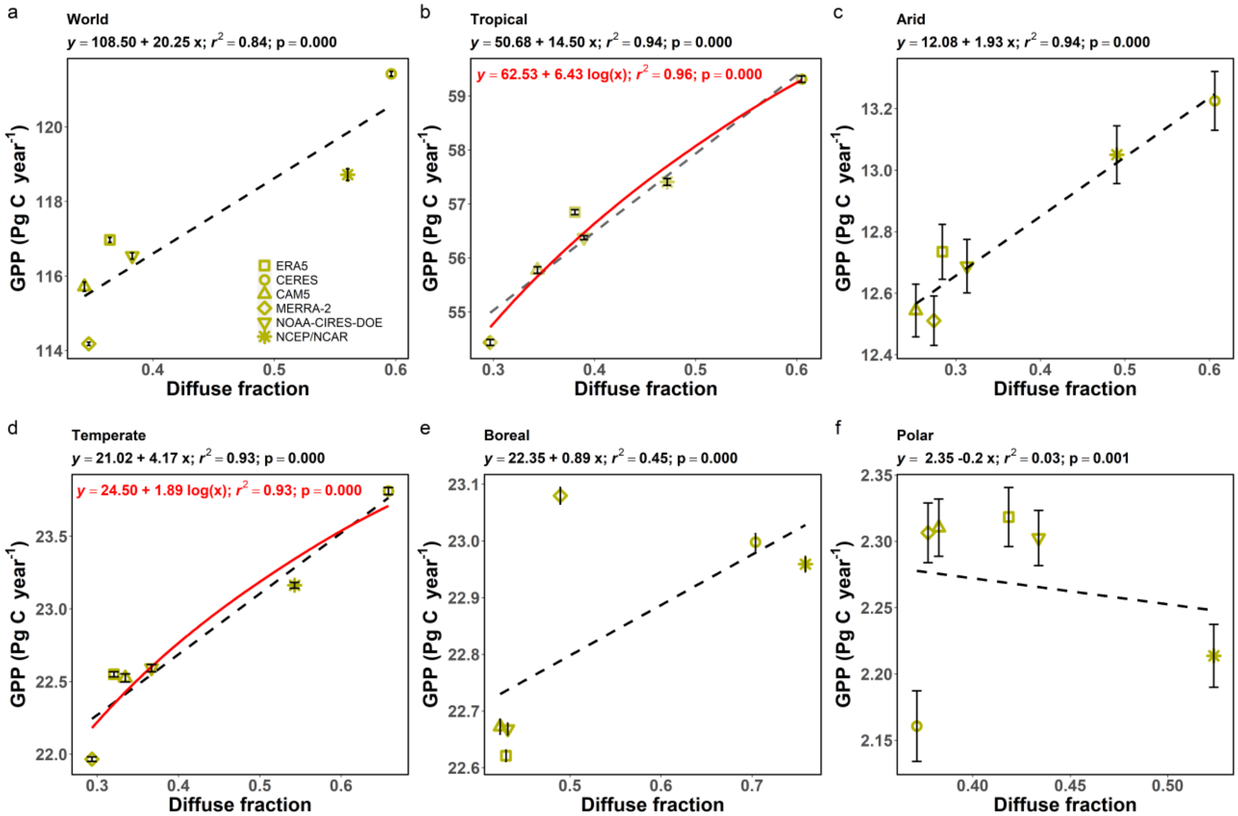

Figure S10 Response of gross primary productivity to inter-product diffuse fraction spread for years 30 to 39 of the simulations. Associations between gross primary productivity (GPP) and diffuse fraction (k_d) across different land model simulations forced using k_d from the six products (NCEP/NCAR, NOAA-CIRES-DOE, ERA5, MERRA-2, CERES, and CAM) considered here for (a) all terrestrial surfaces, (b) tropical climate, (c) arid climate, (d) temperate climate, (e) boreal climate, and (f) polar climate for the 10-year period covering years 30 to 39 of the simulation. The lines of best fit and the linear regression equations, with coefficient of determination r^2 and p-values are noted. For tropical and temperate climate, logarithmic fits and associated equations are also noted (in red). The vertical error bars show the inter-annual standard error for the 10-year period.

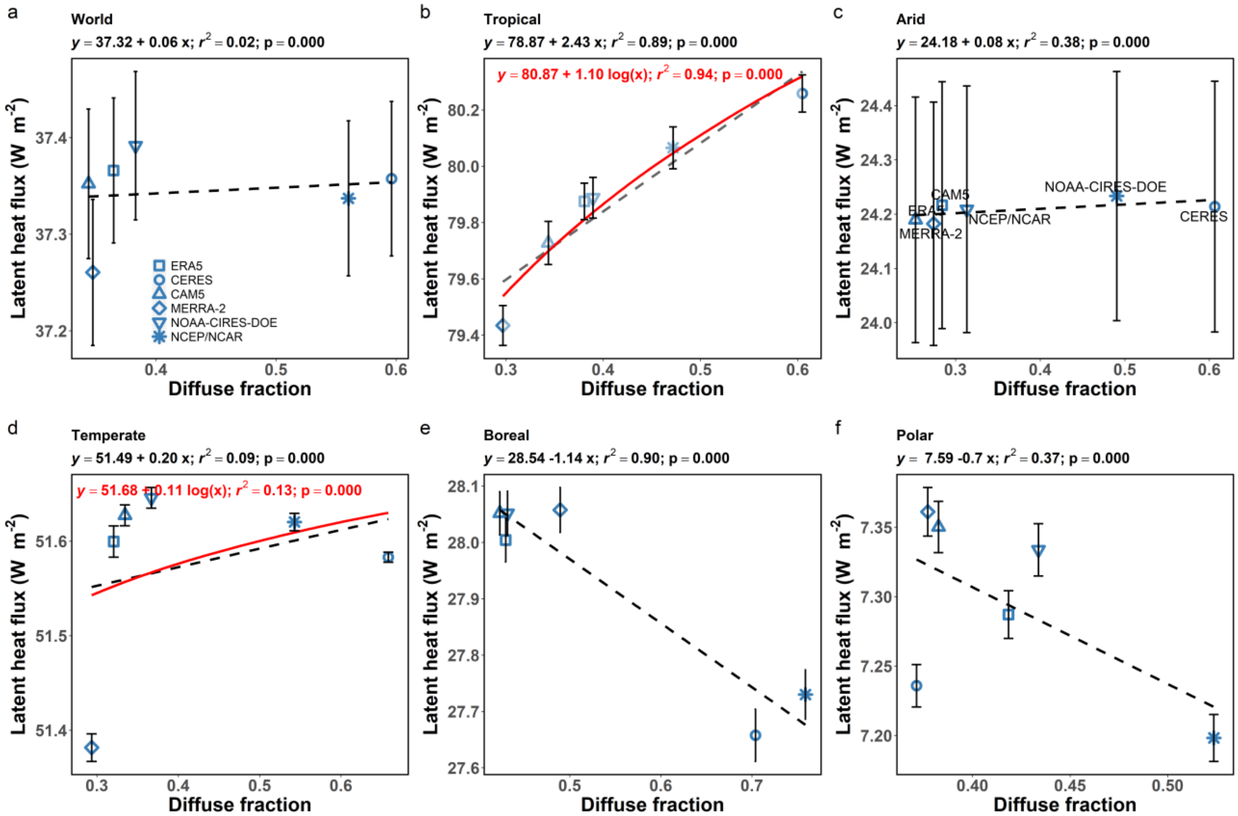

Figure S11 Response of latent heat flux to inter-product diffuse fraction spread for years 30 to 39 of the simulations. Associations between latent heat flux and diffuse fraction (k_d) across different land model simulations forced using k_d from the six products (NCEP/NCAR, NOAA-CIRES-DOE, ERA5, MERRA-2, CERES, and CAM) considered here for (a) all terrestrial surfaces, (b) tropical climate, (c) arid climate, (d) temperate climate, (e) boreal climate, and (f) polar climate for the 10-year period covering years 30 to 39 of the simulation. The lines of best fit and the linear regression equations, with coefficient of determination r^2 and p-values are noted. For tropical and temperate climate, logarithmic fits and associated equations are also noted (in red). The vertical error bars show the inter-annual standard error for the 10-year period.

Table S1 Summary of AmeriFlux sites considered here, along with their location, elevation, and underlying land cover class. ENF=Evergreen Needleleaf Forest; GRA=Grassland; CRO=Cropland; DBF=Deciduous Broadleaf Forest; MF= Mixed Forest; OSH=Open Shrubland; WET= Permanent wetland

Site Name	Latitude	Longitude	Elevation	Land cover
US-A32	36.81927	-97.8198	335	GRA
US-A74	36.80846	-97.5489	337	CRO
US-ARM	36.6058	-97.4888	314	CRO
US-Bi2	38.109	-121.535	-4.98	CRO
US-HB2	33.3242	-79.244	4.7	ENF
US-MRf	44.64649	-123.551	263	ENF
US-xAB	45.76243	-122.33	363	ENF
US-xBN	65.15401	-147.503	263	ENF
US-xBR	44.06388	-71.2873	232	DBF
US-xCP	40.8155	-104.746	1654	GRA
US-xDC	47.16165	-99.1066	559	GRA
US-xDJ	63.88112	-145.751	529	ENF
US-xDL	32.54172	-87.8039	22	MF
US-xGR	35.68896	-83.502	579	DBF
US-xHA	42.5369	-72.1727	351	DBF
US-xHE	63.87569	-149.213	705	OSH
US-xJE	31.19484	-84.4686	44	ENF
US-xJR	32.59068	-106.843	1329	OSH
US-xKA	39.11044	-96.613	1329	GRA
US-xKZ	39.10077	-96.5631	381	GRA
US-xNG	46.76972	-100.915	578	GRA
US-xNQ	40.17759	-112.452	1685	OSH
US-xRM	40.27591	-105.546	2743	ENF
US-xSE	38.89008	-76.56	15	DBF
US-xSL	40.4619	-103.029	1364	CRO
US-xSP	37.03337	-119.262	1160	ENF
US-xSR	31.91068	-110.835	983	OSH
US-xST	45.50894	-89.5864	481	DBF
US-xTE	37.00583	-119.006	2147	ENF
US-xTL	68.66109	-149.37	843	WET
US-xTR	45.49369	-89.5857	472	DBF
US-xUK	39.04043	-95.1922	335	DBF
US-xUN	46.23388	-89.5373	518	MF
US-xWD	47.12823	-99.2414	579	GRA
US-xWR	45.82049	-121.952	407	ENF
US-xYE	44.95348	-110.539	2116	ENF

Table S2 Summary of FLUXNET sites considered here, along with their location, elevation, and underlying land cover class. ENF=Evergreen Needleleaf Forest; GRA=Grassland; CRO=Cropland; DBF=Deciduous Broadleaf Forest; MF= Mixed Forest; OSH=Open Shrubland; WET= Permanent wetland

Site Name	Latitude	Longitude	Elevation	Land cover
CZ-BK1	49.50208	18.53688	875	ENF
CZ-BK2	49.49443	18.54285	855	GRA
DE-Geb	51.09973	10.91463	161.5	CRO
DE-Hai	51.07921	10.45217	430	DBF
DE-Lnf	51.32822	10.3678	451	DBF
DE-Tha	50.96256	13.56515	385	ENF
FI-Hyy	61.84741	24.29477	181	ENF
FR-Gri	48.84422	1.95191	125	CRO
FR-LBr	44.71711	-0.7693	61	ENF
IT-Ren	46.58686	11.43369	1730	ENF
RU-Che	68.61304	161.3414	6	WET
NL-Hor	52.24035	5.0713	2.2	GRA

Table S3 Summary of observed net ecosystem exchange at AmeriFlux sites divided into low (k_d<0.35) and high (k_d>0.65) k_d regimes for different bins of absorbed shortwave radiation at the surface (K_{abs}). Differences in net ecosystem exchange between the regimes that are statistically significant (p<0.01) are in bold and cases where not enough data are available to perform (a) two-tailed t-test are in grey.

	Net ecosystem exchange (μmol CO_2 m^{-2} s^{-1})									
K_{abs} bins	**100-200 W m^{-2}**		**200-300 W m^{-2}**		**300-400 W m^{-2}**		**400-500 W m^{-2}**		**500-600 W m^{-2}**	
Site Name	**k_d<0.35**	**k_d>0.65**	**k_d<0.35**	**k_d>0.65**	**k_d<0.35**	**k_d>0.65**	**k_d<0.35**	**k_d>0.65**	**k_d<0.35**	**k_d>0.65**
US-A32	**-0.98**	**-1.75**	**-2.67**	**-5.45**	**-4.5**	**-8.17**	**-6.1**	**-12.48**	-9.24	-11.77
US-A74	**0**	**-0.7**	-0.72	-1.28	-1.59	-2.48	-2.61	-3.82	-3.4	-5.02
US-ARM	NaN	NaN	NaN	NaN	NaN	NaN	NaN	NaN	NaN	NaN
US-Bi2	NaN	NaN	NaN	NaN	NaN	NaN	NaN	NaN	NaN	NaN
US-HB2	NaN	NaN	NaN	NaN	NaN	NaN	NaN	NaN	NaN	NaN
US-MRf	**-1.83**	**-6.16**	**-4.49**	**-12.18**	**-7.23**	**-17.1**	**-9.82**	**-20.47**	**-11.71**	**-22.68**
US-xAB	**-0.55**	**-3.24**	**-2.74**	**-5.39**	**-4.04**	**-7.74**	-4.92	-10.98	-5.32	NaN
US-xBN	0.66	-1.1	**-0.29**	**-3.07**	**-0.38**	**-2.5**	-0.89	NaN	-1.54	NaN
US-xBR	**-0.85**	**-2.76**	**-2.83**	**-8.93**	**-5.39**	**-12.47**	**-8.45**	**-14.9**	**-10.5**	**-16.32**
US-xCP	-0.57	-0.07	-0.74	-0.32	-1.13	-1.43	-1.13	-1.96	-1.85	-1.55
US-xDC	NaN	NaN	0.06	-0.54	NaN	NaN	NaN	-1.07	NaN	NaN
US-xDJ	NaN	NaN	NaN	NaN	NaN	NaN	NaN	NaN	NaN	NaN
US-xDL	-0.85	-0.49	-3.51	-4.61	**-5.26**	**-8.17**	**-5.73**	**-14.07**	**-6.69**	**-22.84**
US-xGR	-3.37	NaN	NaN	NaN	NaN	NaN	-1.72	NaN	NaN	NaN
US-xHA	2.28	NaN	-27.4	NaN	-6.41	NaN	NaN	NaN	-27.24	NaN
US-xHE	NaN	0.39	NaN	NaN	NaN	NaN	NaN	NaN	NaN	NaN
US-xJE	NaN	NaN	NaN	-3.26	-2.37	NaN	-13.36	NaN	NaN	NaN
US-xJR	-1.05	NaN	-0.03	NaN	NaN	NaN	NaN	NaN	NaN	NaN
US-xKA	0.16	1.94	-1.1	3.76	-3.74	1.82	0.28	-8.01	-2.25	-7.82
US-xKZ	NaN	NaN	NaN	NaN	NaN	NaN	NaN	NaN	-5.16	NaN
US-xNG	-0.26	-0.57	NaN	NaN	NaN	NaN	NaN	NaN	NaN	NaN
US-xNQ	NaN	NaN	NaN	NaN	NaN	NaN	NaN	NaN	NaN	NaN
US-xRM	**-0.03**	**-0.94**	**-0.78**	**-1.81**	**-0.81**	**-2.77**	**-1.42**	**-5.2**	**-2.61**	**-6.81**
US-xSE	NaN	NaN	NaN	NaN	NaN	NaN	NaN	NaN	NaN	NaN

US-xSL	NaN	NaN	-0.53	NaN	NaN	NaN	NaN	NaN	NaN	NaN
US-xSP	1.66	NaN	NaN	NaN	NaN	NaN	NaN	NaN	-2.07	NaN
US-xSR	0.67	1.13	0.04	0.27	0.33	0.56	0.09	-0.24	0.07	-0.54
US-xST	NaN	-6.8	NaN	NaN	NaN	-21.91	NaN	-15.16	NaN	NaN
US-xTE	-1.07	NaN	-1.46	NaN	-1.68	NaN	NaN	-4.35	NaN	-3.82
US-xTL	NaN	NaN	NaN	NaN	NaN	NaN	NaN	NaN	NaN	NaN
US-xTR	0.91	-3.24	-6.21	0.39	2.14	-1.65	-1.37	-13.25	-3.03	NaN
US-xUK	0.89	-3.15	4.54	-9.31	-4.72	-11.99	-7.33	-13.37	-6.81	NaN
US-xUN	-14.19	NaN	NaN	-10.23	-4.3	**-18.93**	**0.32**	-20.64	-11.72	NaN
US-xWD	**0.19**	**-0.84**	**-1.08**	**-3.52**	**-2.3**	**-5.78**	**-3.05**	**-6.3**	**-4.16**	**-7.61**
US-xWR	-0.36	-5.01	**0.5**	**-9.29**	-6.68	-8.51	**-7.47**	**-19.47**	**-8.46**	**-14.88**
US-xYE	**-0.17**	**-2.38**	**-0.73**	**-3.04**	**-2.08**	**-5.18**	**-2.99**	**-7.19**	-3.48	-9.09

Table S4 Summary of observed latent heat flux at AmeriFlux sites divided into low (k_d<0.35) and high (k_d>0.65) k_d regimes for different bins of absorbed shortwave radiation at the surface (K_{abs}). Differences in latent heat flux between the regimes that are statistically significant (p<0.01) are in bold and cases where not enough data are available to perform (a) two-tailed t-test are in grey.

	Latent heat flux (W m^{-2})									
K_{abs} bins	**100-200 W m^{-2}**		**200-300 W m^{-2}**		**300-400 W m^{-2}**		**400-500 W m^{-2}**		**500-600 W m^{-2}**	
Site Name	**k_d<0.35**	**k_d>0.65**	**k_d<0.35**	**k_d>0.65**	**k_d<0.35**	**k_d>0.65**	**k_d<0.35**	**k_d>0.65**	**k_d<0.35**	**k_d>0.65**
US-A32	64.25	61.4	87.19	94.08	**106.37**	**128.93**	**137.1**	**174.82**	**186.35**	**209.22**
US-A74	68.76	73.38	98.31	105.95	124.98	136.66	**150.74**	**176.89**	170.9	205.43
US-ARM	**50.93**	**62.35**	**81.1**	**97.08**	**98.83**	**132.68**	**125.91**	**168.81**	**179.8**	**208.53**
US-Bi2	NaN	44	**138.24**	**71.32**	**117.26**	**89.61**	**120.34**	**115.62**	**148.35**	**175.72**
US-HB2	**48.81**	**77.32**	**68.54**	**97.02**	**101.09**	**116.95**	**122.19**	**146.06**	**147.08**	**181.18**
US-MRf	**57.14**	**41.9**	66.55	64.88	**80.67**	**96.39**	**104.4**	**116.32**	**124.13**	**134.72**
US-xAB	32.5	34	59.01	61.46	97.95	103.89	131.76	99.66	197.57	NaN
US-xBN	22.83	22.26	38.99	54.39	**45.49**	**76.56**	70.98	NaN	77.56	NaN
US-xBR	**40.5**	**51.76**	**61.98**	**84.77**	**85.52**	**117.73**	**118.12**	**160.77**	**150.55**	**173.53**
US-xCP	**21.89**	**33.2**	41.18	38.13	53.75	74.42	60.15	90.54	88.88	100.41
US-xDC	NaN	NaN	32.89	37.25	NaN	NaN	NaN	69.21	NaN	NaN
US-xDJ	NaN	NaN	NaN	NaN	NaN	NaN	NaN	NaN	NaN	NaN
US-xDL	**42.03**	**55.14**	78.28	90.69	**108.74**	**128.5**	**144.75**	**177.2**	**174.92**	**270.89**
US-xGR	22.49	NaN	NaN	NaN	NaN	NaN	26.88	NaN	NaN	NaN
US-xHA	10.06	NaN	96.64	NaN	67.42	NaN	NaN	NaN	250.58	NaN
US-xHE	NaN	29.95	NaN	NaN	NaN	NaN	NaN	NaN	NaN	NaN
US-xJE	NaN	NaN	NaN	108.4	153.31	NaN	153.91	NaN	NaN	NaN
US-xJR	50.65	NaN	35.58	NaN	NaN	NaN	NaN	NaN	NaN	NaN
US-xKA	39.69	41.15	63.52	65.76	91.75	88.57	114.3	113.32	138.86	155.36
US-xKZ	NaN	NaN	NaN	NaN	NaN	NaN	NaN	NaN	168.82	NaN
US-xNG	8.92	14.95	NaN	NaN	NaN	NaN	NaN	NaN	NaN	NaN
US-xNQ	NaN	NaN	NaN	NaN	NaN	NaN	NaN	NaN	NaN	NaN
US-xRM	**29.03**	**41.99**	**41.96**	**59.19**	**54.8**	**77.72**	**67.97**	**99.35**	**95.15**	**117.51**
US-xSE	NaN	NaN	NaN	NaN	NaN	NaN	NaN	NaN	NaN	NaN

US-xSL	NaN	NaN	47.18	NaN	NaN	NaN	NaN	NaN	NaN	NaN
US-xSP	7.03	NaN	NaN	NaN	NaN	NaN	NaN	NaN	74.92	NaN
US-xSR	**13.76**	**35.27**	**21.05**	**42.87**	**24.74**	**44.79**	**27.45**	**50.66**	**35.68**	**74.42**
US-xST	NaN	35.12	NaN	NaN	NaN	136.49	NaN	176.46	NaN	NaN
US-xTE	53.95	NaN	43.53	NaN	61.48	NaN	NaN	83.86	NaN	135.93
US-xTL	NaN	NaN	NaN	NaN	NaN	NaN	NaN	NaN	NaN	NaN
US-xTR	**2.28**	**56.44**	**52.16**	**12**	**28.75**	**20.26**	**52.68**	**231.33**	85.1	NaN
US-xUK	68.35	55.85	63.74	83.56	94.36	89.26	119.08	159.31	139.69	NaN
US-xUN	36.51	NaN	NaN	193.94	**70.15**	**252.92**	**3.32**	**217.32**	158.48	NaN
US-xWD	**12.48**	**24.09**	**44.34**	**66.03**	**78.37**	**92.31**	**104.23**	**116.84**	**145.91**	**166.46**
US-xWR	40.54	53.88	**54.27**	**104.58**	**64.34**	**99.03**	113.31	156.74	141.64	192.82
US-xYE	34.24	67.35	51.18	84.4	**52.26**	**118.88**	**93.39**	**172.32**	163.06	177.62

Table S5 Summary of observed gross primary productivity at FLUXNET sites divided into low (k_d<0.35) and high (k_d>0.65) k_d regimes for different bins of absorbed shortwave radiation at the surface (K_{abs}). Differences in gross primary productivity between the regimes that are statistically significant (p<0.01) are in bold and cases where not enough data are available to perform (a) two-tailed t-test are in grey.

	Gross primary productivity (µmol CO_2 m^{-2} s^{-1})									
K_{abs} bins	**100-200 W m^{-2}**		**200-300 W m^{-2}**		**300-400 W m^{-2}**		**400-500 W m^{-2}**		**500-600 W m^{-2}**	
Site Name	**k_d<0.35**	**k_d>0.65**	**k_d<0.35**	**k_d>0.65**	**k_d<0.35**	**k_d>0.65**	**k_d<0.35**	**k_d>0.65**	**k_d<0.35**	**k_d>0.65**
CZ-BK1	**10.26**	**11.22**	**13.65**	**16.07**	**16.45**	**19.36**	**18.33**	**21.42**	**20.06**	**23.43**
CZ-BK2	6.85	6.91	9	9.38	10.42	11.35	**10.44**	**12.32**	**11.12**	**13.09**
DE-Geb	**4.17**	**5.33**	**6.33**	**8.68**	**8.34**	**11.91**	**10.39**	**13.99**	**12.77**	**16.67**
DE-Hai	**6.89**	**8.59**	**9.54**	**14.23**	**12.85**	**18.39**	**16.4**	**21.4**	**18.7**	**26.4**
DE-Lnf	**6.94**	**8.89**	**9.2**	**14.26**	**11.63**	**18.46**	**14.62**	**21.99**	**17.11**	**24.74**
DE-Tha	8.75	7.5	8.96	10.78	**8.14**	**13.21**	**6.6**	**14.98**	**11.1**	**18.17**
FI-Hyy	**5.99**	**6.91**	**7.88**	**10.43**	**9.62**	**12.9**	**11.52**	**15.21**	**13.45**	**16.92**
FR-Gri	**6.02**	**6.85**	**8.06**	**11.48**	**10.79**	**15.23**	**14.21**	**17.35**	17.48	17.15
FR-LBr	**7.85**	**7.7**	**10.18**	**10.94**	**12.08**	**13.34**	**13.39**	**15.65**	**13.47**	**17.39**
IT-Ren	**5.3**	**6.78**	**6.69**	**10.53**	**7.89**	**14.1**	**10.97**	**16.77**	**14.08**	**19.73**
NL-Hor	8.37	NaN	12.02	NaN	15.1	NaN	16.94	NaN	18.58	NaN

Table S6 Summary of observed latent heat flux at FLUXNET sites divided into low (k_d<0.35) and high (k_d>0.65) k_d regimes for different bins of absorbed shortwave radiation at the surface (K_{abs}). Differences in latent heat flux between the regimes that are statistically significant (p<0.01) are in bold and cases where not enough data are available to perform (a) two-tailed t-test are in grey.

	Latent heat flux (W m^{-2})									
K_{abs} bins	**100-200 W m^{-2}**		**200-300 W m^{-2}**		**300-400 W m^{-2}**		**400-500 W m^{-2}**		**500-600 W m^{-2}**	
Site Name	**k_d<0.35**	**k_d>0.65**	**k_d<0.35**	**k_d>0.65**	**k_d<0.35**	**k_d>0.65**	**k_d<0.35**	**k_d>0.65**	**k_d<0.35**	**k_d>0.65**
CZ-BK1	**30.41**	**34.63**	**52.42**	**65.41**	**75.38**	**91.31**	**98.46**	**116.3**	**125.57**	**129.13**
CZ-BK2	29.69	22.78	51.43	45.63	74.77	67.38	97.71	103.32	124.09	125.71
DE-Geb	**33.69**	**37.15**	**59.58**	**73.44**	**88.48**	**110.99**	**119.57**	**142.65**	**154.68**	**176.56**
DE-Hai	**45.14**	**50.31**	**79.44**	**97.25**	**113.63**	**139.74**	**151.12**	**166.11**	186.16	205.35
DE-Lnf	**34.86**	**45.95**	**59.22**	**93.23**	**88.30**	**138.16**	**124.99**	**172.22**	**165.01**	**193.32**
DE-Tha	39.98	30.21	53.25	44.69	50.95	66.6	**46.68**	**83.43**	**78.09**	**116.87**
FI-Hyy	**32.13**	**43.44**	**51.51**	**77.55**	**75.66**	**104.38**	**105.87**	**130.39**	**139.35**	**161.11**
FR-Gri	**38.78**	**52.12**	**62.23**	**88.88**	**96.14**	**118.39**	**132.43**	**146.64**	**168.36**	**168.87**
FR-LBr	**41.97**	**56.8**	**68.28**	**94.4**	**95.26**	**125.54**	**125.75**	**153.49**	**146.37**	**178.57**
IT-Ren	**35.97**	**60.5**	**56.93**	**103.33**	**79.69**	**154.57**	**113.51**	**178.3**	**158.18**	**215.61**
NL-Hor	75.53	NaN	147.64	NaN	199.62	NaN	256.23	NaN	312.89	NaN